ACOUSTIC EMISSION DURING STRESS CORROSION CRACKING TEST

Mikio Takemoto, Aoyama Gakuin University
Hideo Cho, Aoyama Gakuin Univ.

ABSTRACT

AE monitoring from various types of stress corrosion cracking (SCC) has been conducted for the past 15 years in our laboratory. This paper discusses AE results of active-path dissolution-type SCC of austenitic stainless steel in chloride solution and fused salt, fluoride and polythionic acid solutions, brass in ammonia (Mattosson's solution), and carbon steels in nitrite solution. Transgranular-type SCC of 304 steel in concentrated chloride solution did not produce AEs, but intergranular SCC of sensitized 304 steel in chloride, polythionic acid and fluoride solutions did produce AEs. Intergranular SCC of brass in Mattosson's solution and carbon steel in nitirate solution did not.

Keywords: Active path corrosion, stress corrosion cracking, transgranular SCC, intergranular SCC, delayed fracture, fracture dynamics

INTRODUCTION

Stress corrosion cracking (SCC) is important engineering problem in various industries. SCC of austenitic stainless steels in chloride–containing solution and in high temperature light water of nuclear power plant often resulted in serious disasters and economical damages. Monitoring of SCC by remote sensing technique such as acoustic emission is strongly needed in various fields. AE monitoring from SCC can make a contribution to the mechanistic study of SCC. It is not, however, well understood whether SCC produces AE.

Definition and interpretation of the SCC appears to be different among engineers and researchers in different countries. Delayed fracture of high tension ferritic steel is well known to produce strong AEs. This fracture is accelerated by cathodic polarization, or tends to occurs in cathodic (active) potential range where hydrogen cations can exist on the surface. Contrary to this, SCC can be prevented by the cathodic polarization. It occurs in a limited anodic potential range. We (Japanese corrosion engineers) separate the SCC from the delayed fracture (hydrogen induced cracking). From the fact that SCC occurs in a limited anodic potential range, SCC is often called as the active-path corrosion (APC) type SCC. This means that SCC is caused by the anodic dissolution of metal along the active paths such as slip lines, grain boundaries and lath-martensites, and not by the mechanical brittle fracture. As long as the SCC is caused by anodic dissolution of metal, it does not produce strong AEs. Thus the "cracking" of the term "SCC " designates the fine opening displacement looks like "crack" as a result of anodic dissolution of metal, but not the mechanical fracture.

Some researchers[1] proposed alternate SCC mechanism such as two-step progression assisted by delayed fracture. Strain-induced lath-martensite can play an important role in the two-step model.

Okada first studied AE from SCC and concluded that SCC of austenitic stainless steel in chloride solution did not produce strong AEs, but delayed fracture did produce strong AEs. This research suggests the feasibility of APC for chloride SCC of 304 steel. No reliable data is, however, absent for SCC mechanism. Researchers [2][3][4]for SCC of binary alloys which produce de-alloyed brittle surface film are against the APC mechanism, since an extremely high anodic current density of $30A/cm^2$, corresponding to the SCC propagation rate of 360 mm/h can not be achieved by electrochemical reaction. Kelly [5]proposed "film induced fracture (FIF)" model for explaining the fast SCC velocity of $18x10^6$ mm/h for Ag-Au alloy in 1M $HClO_4$ solution.

We studied SCC mechanism using AE for last 15 years. These SCCs involve 1) transgranular SCC (abbreviated as TG-SCC) of non-sensitized austenitic stainless steel 304 in 35mass % $MgCl_2$ solution, 2) Intergranular SCC (IG-SCC) of sensitized 304 steel in $MgCl_2$ solution, 3) IG-SCC of 304 steel by molten mixed salt at 873K, 4) IG-SCC of sensitized 304 steel in polythionic and fluoride containing solution at room temperature, 5) IG-SCC of low carbon steel in hot nitrite solution and 6)IG-SCC of brass in ammonia or Mattsson's solution.

Foe the metal-environment system which produces SCC-related AEs, fracture dynamics were studied by waveform matching. These analyses involve bulk-wave AEs for test 3) and 4), Lamb-wave AEs for 1), 2) and 5), cylinder wave for 6). The system 4) and 5) are the SCC of metals which produce thick passivation film of magnetite and tarnish film, respectively. SCC test of 4) and 5) produce a number of AEs, but most AEs are diagnosed to be from the fracture of thick passivation film

TRANGRANULAR SCC OF NON-SENSITIZED AUSTENITIC SATINLESS STEEL 304 IN CONCENTRATED CHLORIDE SOLIUTION

TG-SCC by chloride solution is the most popular SCC experienced in chemical and petro-chemical plants. We studied AEs from non-sensitized 304 steel in 35mass % $MgCl_2$ solution at 383 K (non-boiling temperature). This solution shows pH=2.9 and does not evolve hydrogen gas. IN the test, SCCs were produced by changing tensile stress levels of plate specimens in a isothermal solution. Two types of AE sensor, PAC PICO and JT TOSHI M204 with a head amplifier of 30 dB were utilized. We conducted several tests, however, could not detect any AEs at even 80 dB amplification as long as SCC is trasngranular. This results was reported at 15th IAES[6].

INTERGRANULAR SCC OF SENSITIZED 304 STEEL UNDER HEAT FLUX

It has been well recognized that the concentrated magnesium chloride solution such as 42 mass % at boiling temperature (418 K) does not cause IG-SCC even the steel is sensitized. We found that IG-SCC could be produced by using moderate magnesium chloride solution at relatively low temperatures. Multi-axial stress states, by superposing thermal stress to mechanical tensile loading, can accelerates IG-SCC. We monitored both the AEs and electrochemical noises during SCC test of sensitized 304 plate in 38mass % $MgCl_2$ solution under heat-flux. As shown in Fig. 1, 38 mass % $MgCl_2$ solution in a vertical corrosion cell was heated to 363 K (non-boiling temperature) by an infrared lamp. pH of this solution is above 2.5 and does not produce hydrogen gas bubbles. AE was monitored by four PICO sensors mounted at four corners of 110 mm and 40 mm square. Sensor outputs are amplified by 40dB. Fluctuation of corrosion potential was monitored at micro-volt order by a reference electrode of Ag/AgCl and a digital potentiometer. AE and corrosion potential data were

simultaneously stored in a computer.

Hagyard et.al., [7]first reported potential fluctuations by pitting, crevice corrosion and SCC. The fluctuation is induced by electrochemical non-faradic reaction, and can be explained by assuming double-layer capacitance produced on the electrode surface. Inoue[8] experimentally demonstrated two types of corrosion potential fluctuation. One is the RD type or rapid drop (rapid shift to active) followed by slow recovery, and another the RR or rapid rise (rapid shift to noble) followed by slow recovery. RD type fluctuation is induced by pitting and SCC which shows rapid increase of anodic current, while the RR by crevice corrosion in reducing environment which shows rapid increase of cathodic current. Monitoring of potential fluctuation gives us important information of corrosion behavior of metals in a given environment.

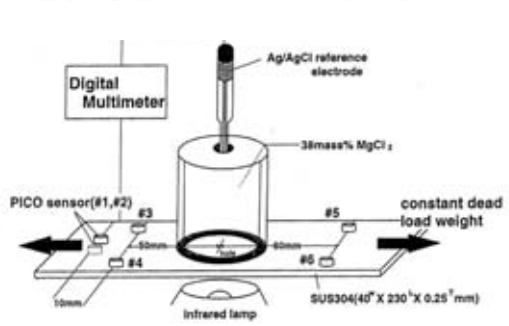

Fig.1 Test method for IG-SCC of 304 steel under heat flux

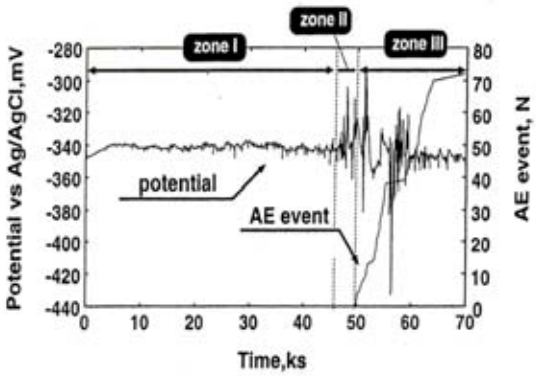

Fig.2 Change of corrosion potential and AE event count with test time of SCC

As the vertical corrosion cell is attached onto the plate specimen via a O-ring, both the crevice corrosion under the O-ring and SCC occurs in the method shown in Fig.1. We measured AE and potential fluctuation at 180 MPa by dead-load system. Figure 2 shows the change of corrosion potential and AE event counts with time.

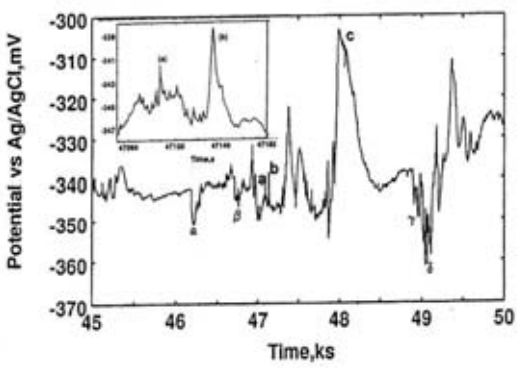

Fig.3 RR type potential fluctuation in Zone I

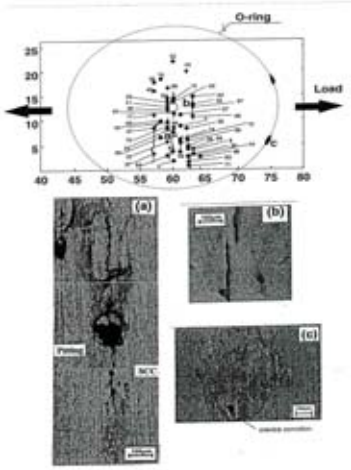

Fig. 5 Surface SCC with pitting corrosion and AE sources

Zone I shows only small amplitude RD type potential fluctuation (Fig.3) and does not produce any AE. In the Zone II, amplitude of potential fluctuation increased, while AE was not detected. Potential fluctuation in Zone II was typical RR type and indicates the occurrence of crevice corrosion under the O-ring. In Zone III, we detected AEs and RD type potential fluctuation as shown in Fig 5.

Triangles near the potential curve show the AE timing,

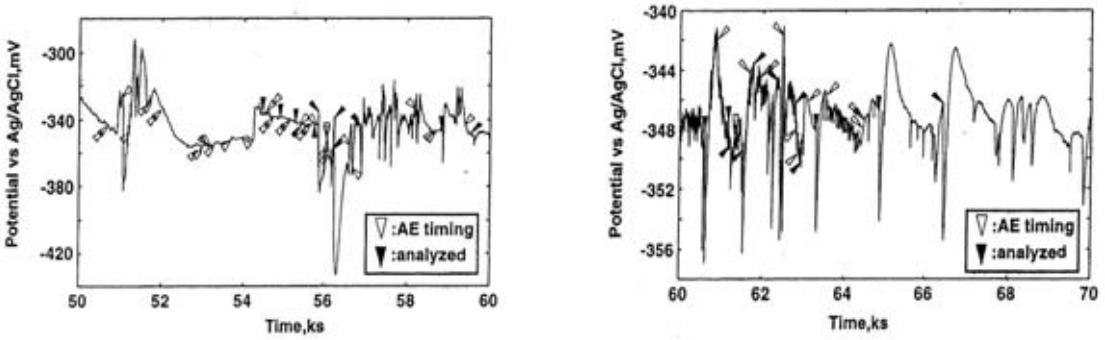

Fig.4 RD type potential fluctuation and AE timing in Zone III

Figure 5 shows surface cracks and source location of AE events. AE sources were located along the SCC. Here the source of Lamb wave AEs were determined by virtual source scanning of the first arrival times of the So-mode since IG-SCC produced Lamb wave AE with sufficient amplitude of So-mode. IG-SCCs were associated with pits. (photos (a) and (b)). There observed crevice corrosion under the O-ring (photo (c)). These corrosion morphologies agree well with the potential fluctuations detected during the test.

We studied correspondence of potential shift and AE timing. Figure 6 shows timing of RD type potential shift and AE timing (solid triangle) in the left and waveform matching of So-mode AE. It can be seen that the potential shifts to the active direction when AE is detected. This indicates that the brittle fracture along grain boundary induced rapid anodic current in the corrodant impregnated into the crack. Waveform matching of the So-packet represented the fracture parameter of Fig. 7. Maximum crack generation time is estimated as 43 m/s which has not been reported for chloride SCC so far. We can conclude that IG-SCC of stainless steel by chloride anion produces fast grain boundary crack and AEs.

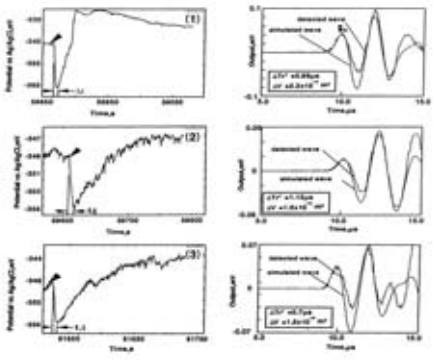

Fig.6 Timing of potential fluctuation and AE in Zone III and Lamb waveform matching

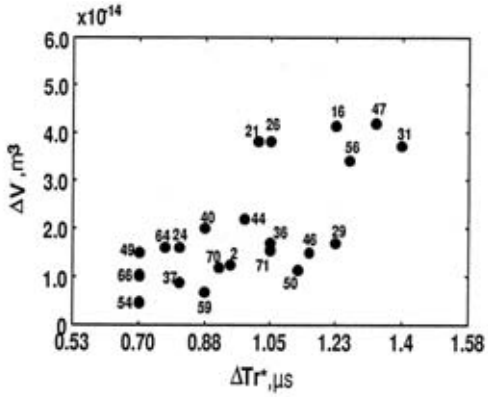

Fig. 7 Fracture parameter of IG-SCC

INTERGRANULAR SCC OF 304 STEEL BY MOLTED SALT AT 873K

Type 304 steel suffers grain boundary attack by molten salt at elevated temperature. This is called as the high temperature SCC. We monitored AEs from 304 steel rod exposed to a mixed salt of 40 mol $PbCl_2$+30%$FeCl_2$+20%NaCl+20%KCl at 873 K, utilizing the method in Fig.8 . We developed a heat-resistant capacitive sensor with alumina film and monitored the bulk wave AE without using

wave guide. As shown in Fig. 9, this system shows IG crack with many fallen-off grains near the crack, which is similar to the features of IG-SCC by polythionic and fluoride solution. Two types of AE were detected as shown in Fig. 10, one is AE with negative polarity of the P-wave due to Mode-I crack and another positive polarity due to mode-II grain boundary gliding. AEs were monitored.

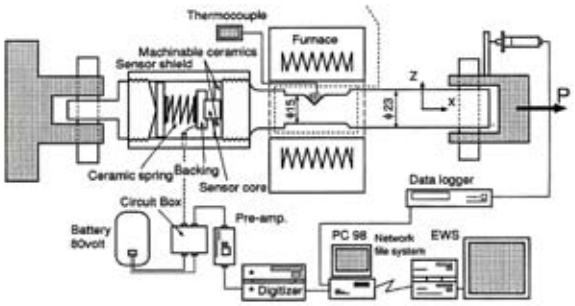

Fig.8 Test method for monitoring of bulk wave AE from SCC by molten

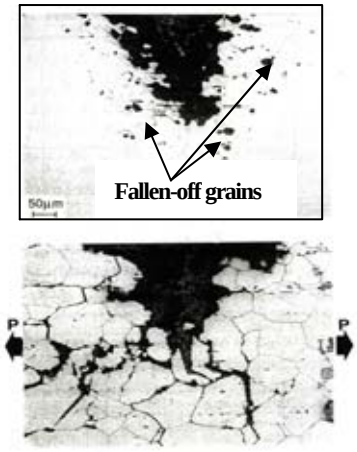

Fig.9 Transverse structure of sensitized 304 steel attacked by molten salt

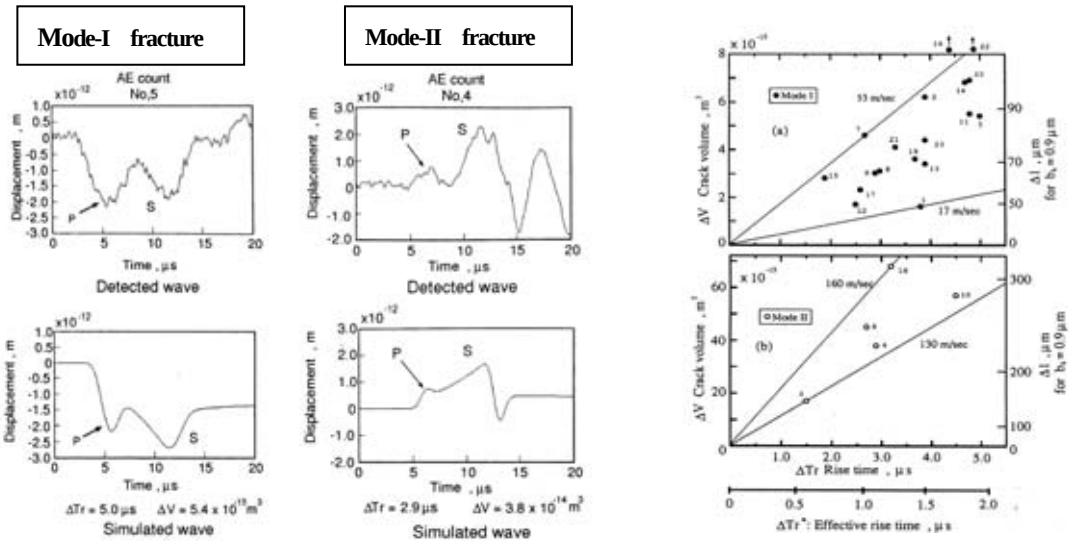

Fig.10 Two types of bulk-wave AEs monitored during molten salt attack test of sensitized 304 steel(the left) and fracture parameters (the right) estimated by waveform matching

IG-SCC OF SENSITIZED 304 STEEL IN POLYTHIONIC AND FLUORIDE CONTAINING SOLUTION AT ROOM TEMPERATURE

Sensitized 304 steel suffers IG-SCC at room temperature in polythionic and fluoride containing solutions. This type of IG-SCC is most catastrophic since of high crack velocity. SCC by polythionic acid (Tetrachionic acid: $H_2S_4O_6$ is the popular chemical composition) has been experienced in petro-refinery plants. Polythionic acid is easily produced by the oxidation of FeS in wet atmosphere. Fluoride ions, possibly induced from wet fumes of shield metal arc welding, also causes severe IG-SCC in sensitized 304 steel at temperatures below 343 K. Sensitization is necessary for both

IG-SCCs. IG-SCCs by these chemicals shows, as shown in Fig. 11, characteristic features of falling-off of the grains near the SCC.

We monitored AEs from IG-SCC of 304 steel sensitized at 873 K for 12 h. Out-of-displacement of the bulk wave AE were monitored using S9208 sensor (#7 sensor) mounted on the the 200% CT specimen (Fig.12). Source location was estimated from arrival time difference of the P-wave monitored by six PICO sensors. WE estimated source dynamics by waveform matching of the out-of-plane displacement of the P-wave. Here, the waveform of the P-wave was computed by convolution of the assumed step-wise crack generation function with the theoretical Green' function of the second kind, and matched to the measured displacement.

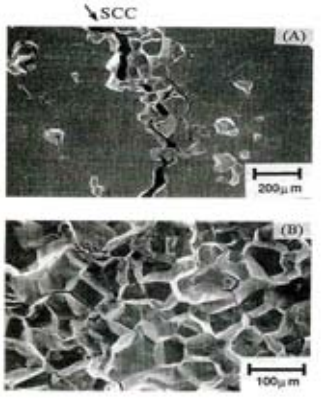

Fig.11 Surface and fracture surface of polythionic SCC of sensitized 304 steel

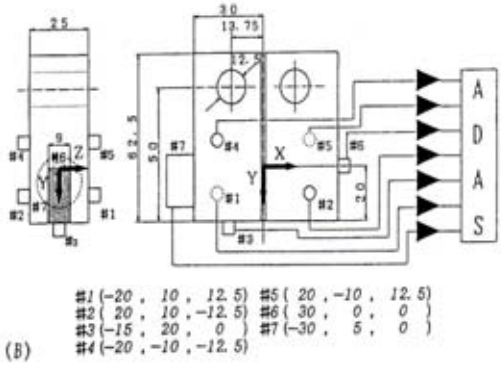

Fig.12 Test method for monitoring AEs from polythionic and fluoride SCC of CT specimen

Figures 13 shows AE timing during constant extension rate SCC test of the CT-specimen in pH=2 $K_2S_4O_6$ and 1000 ppm NaF at room temperature. Sources of 90 % AE events were located in the ligament of the CT-specimen, indicating the AEs from IG-SCCs. Figure 14 shows an example of waveform matching of AE detected for fluoride SCC. The maximum crack velocity is estimated to reach 30 m/s. This velocity corresponds the lowest crack velocity of the delayed fracture of high tension steel, and has not been reported for 304 steel.

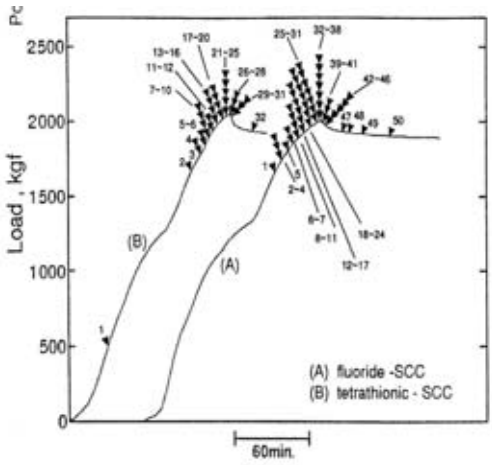

Fig.13 AE timing from IG-SCC of sensitized 304 steel during constant extension rate test

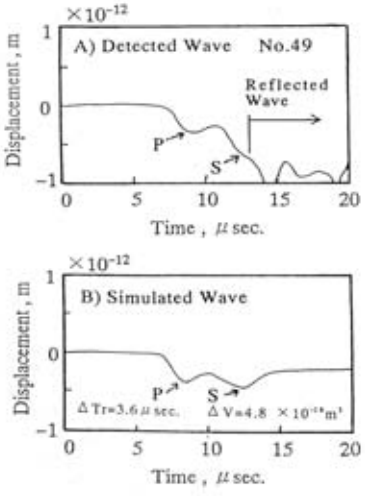

Fig.14 Examples of waveform matching of bulk wave AE detected for IG-SCC by fluoride ions

IG-SCC OF CARBON STEEL IN NITRITE SOLUTION

Carbon steel shows high susceptibility to IG-SCC when its surface was protected by thick magnetite passivation film (up to 60 μm) by oxidation of hot nitrate solution. It must be noted that fractures of the film produces AEs. Uhlig suggested a stress sorption cracking model to this SCC.

We first monitored Lamb-wave AEs from plate specimens with and without magnetite film at being tensile loaded (dead load) in silicone oil at 363K. Result is shown in Fig. 15 . We observed step-wise elongation due to large shear slip across the specimen and associated AEs for the specimen with thick magnetite film, but no AE from the specimen without the film. This clearly indicates that AEs are generated by the fracture of the magnetite film. Continuous type AE indicates continuous fractures of the film.

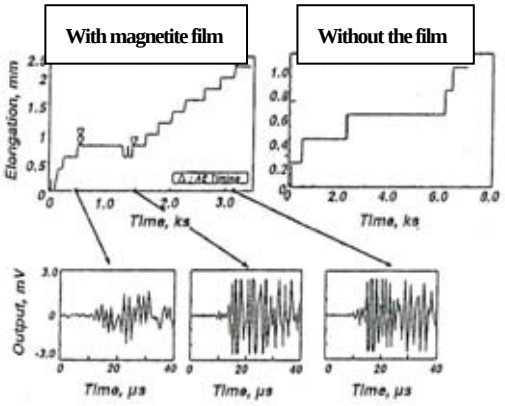

Fig.15 AE from steel plate with and without magnetite film at being loaded in 368 K silicone oil

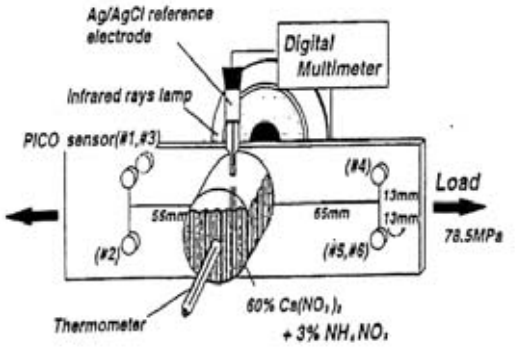

Fig.16 Test method to monitor AE from IG-SCC of carbon steel in hot nitrate solution

We next monitored AEs, potential fluctuation and elongation during SCC test of low carbon steel plate immersed in boiling 3% mass NH_4NO_3 + 60% $Ca(NO_3)_2$ solution by using the equipment of Fig. 16. We monitored a number of AE from early time of the test, as shown in Fig. 17 , however, very few in the zone III in which corrosion potential shifted to active direction and SCC progressed. Lamb wave AEs were classified into four types as shown in the right of Fig.17. Type A,B and D are supposed to be from the film fracture. Only three Type C AEs are possibly from IG-SCC. This means that the nitrate IG-SCC of carbon steel doe not produce sufficient AEs

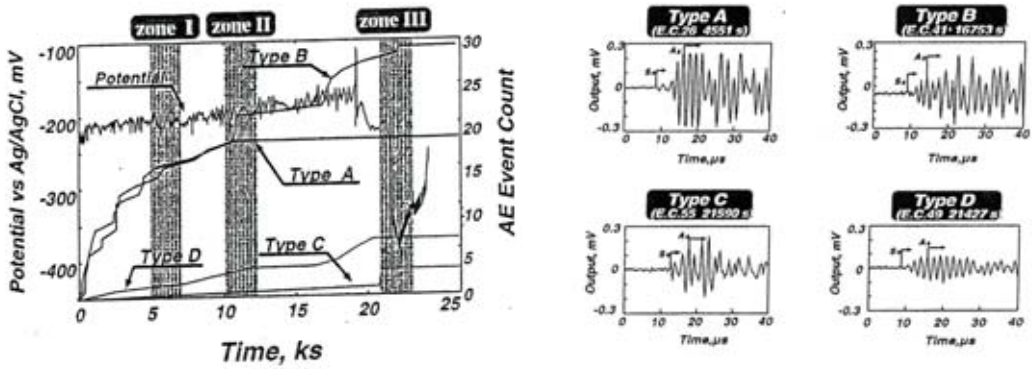

Fig.17 Change of elongation, corrosion potential and AE during IG-SCC of carbon steel in hot nitrate solution

Lamb wave AE. Bulk-wave AE monitoring and analysis are needed.

IG-SCC OF BRAS IN THE MATTOSSON'S SOLUTION

We monitored cylinder wave AEs from IG-SCC of brass tube of 5mm diameter by Mattosson's solution at room temperature. The brass produced thick Cu_2O film, called as the tarnish film, and produces AEs from the film cracking and SCC. One hundred thirteen events were detected before final fracture by IG-SCC for 50 ks. Amplitude of L(0,1) component was too weak to be detected, suggesting film fracture. Bulk wave AE monitoring is needed.

CONCLUSION

We monitored AEs during six kinds of SCC test. These are 1) TG-SCC of non-sensitized austenitic stainless steel 304 in 35mass % $MgCl_2$ solution, 2) IG- SCC of sensitized 304 steel in 38 % $MgCl_2$ solution under heat flux, 3) IG-SCC of 304 steel by molten mixed salt at 873K, 4) IG-SCC of sensitized 304 steel in polythionic and fluoride containing solution at room temperature, 5) IG-SCC of low carbon steel in hot nitrite solution and 6) IG-SCC of brass in Mattosson's solution.

For the SCC of austenitic stainless steel 304, TG-SCC of non-sensitized 304 steel in chloride bearing solution does not produce sufficient AEs. IG-SCC of sensitized 304 steel in chloride solution, molten mixed salt, polythionic and fluoride solutions does produce AEs from SCC. Sensitized 304 steel possesses a feasibility of fast mechanical fracture along grain boundary.

For the IG-SCC of carbon steel in nitrate and brass in mattosson's solution, AEs were supposed to be produced by the fracture of thick film along grain boundary, and possibly not from the SCC. Classification of detected AE signals into AE from SCC and secondary AE from film fracture is difficult for dispersive guided waves.

REFERENCE

[1] E.H.Dix et.al., Trans AIME, 137,11(1940)
[2]E.N.Pugh, Phil.Mag., 13m167(1966)
[3]K.Sieradzki and R.C.Newman., Phil. Mag., A51,95(1985)
[4]A.Paskin and K. Sieradzki, Acta Met., 30,1781(1982) and 31,1253(1983)
[5] R.G.Kelly, Met. Trans., 22A,531(1990)
[6] S.Fujimoyo, M.Takemoto and K.Ono, Progress in AE X, 129(2000)
[7] T.Hagyard and J.R.Williams., Trans. Faraday Soc., 57,295(1961)
[8]H.Inoue, K.Yamakawa, T.Kikuchi and Y.Yoneda, Zairyo-to-Kankyo in Japanese, 45,717(1996)